ATTITUDE CONTROL FOR SATELLITES FLYING IN VLEO

using aerodynamic surfaces

V. CAÑAS MUÑOZ[1], D. GONZÁLEZ[1], J. BECEDAS[1], R. M. DOMÍNGUEZ[1], P. C. E. ROBERTS[2], N. H. CRISP[2], V. T. A. OIKO[2], S. EDMONDSON[2], S. D. WORRALL[2], S. HAIGH[2], K. SMITH[2], R. E. LYONS[2], S. LIVADIOTTI[2], C. HUYTON[2], L. A. SINPETRU[2], S. RODRIGUEZ-DONAIRE[3], D. GARCIA-ALMIÑANA[3], M. NIETO[3], C. MUÑOZ[3], M. SUREDA[3], D. KATARIA[4], G. H. HERDRICH[5], F. ROMANO[5], T. BINDER[5], A. BOXBERGER[5], S. FASOULAS[5], C. TRAUB[5], R. OUTLAW[6], V. HANESSIAN[7], J. MORSBØL[7], R. VILLAIN[8], J. S. PEREZ[8], A. CONTE[8], B. BELKOUCHI[8], A. SCHWALBER[9], B. HEISSERER[9] [1]Elecnor Deimos Satellite Systems, Calle Francia 9, 13500 Puertollano, Spain; [2]The University of Manchester, Oxford Road, Manchester, M13 9PL, UK; [3]UPC-Barcelona TECH, Carrer de Colom 11, 08222 Terrassa, Barcelona, Spain; [4]Mullard Space Science Laboratory (UCL), Holmbury St. Mary, Dorking, RH5 6NT, UK; [5]Institute of Space System, University of Stuttgart, Pfaffenwaldring 29, 70569 Stuttgart, Germany; [6]Christopher Newport University, 1 Avenue of the Arts, Newport News, VA 23606, USA; [7]Gomspace AS, Langagervej 6, 9220 Aalborg East, Denmark; [8]Euroconsult, 86 Boulevard de Sébastopol, 75003 Paris, France; [9]Concentris Research Management GmbH, Ludwigstraße 4, D-82256 Fürstenfeldbruck, Germany

email valentin-jose.canas@deimos-space.com / jonathan.becedas@deimos-space.com

This paper analyses the use of aerodynamic control surfaces, whether passive or active, in order to carry out very low Earth orbit (VLEO) attitude maneuver operations. Flying a satellite in a very low Earth orbit with an altitude of less than 450 km, namely VLEO, is a technological challenge. It leads to several advantages, such as increasing the resolution of optical payloads or increase signal to noise ratio, among others. The atmospheric density in VLEO is much higher than in typical low earth orbit altitudes, but still free molecular flow. This has serious consequences for the maneuverability of a satellite because significant aerodynamic torques and forces are produced. In order to guarantee the controllability of the spacecraft they have to be analyzed in depth. Moreover, at VLEO the density of atomic oxygen increases, which enables the use of air-breathing electric propulsion (ABEP). Scientists are researching in this field to use ABEP as a drag compensation system, and consequently an attitude control based on aerodynamic control could make sense. This combination of technologies may represent an opportunity to open new markets. In this work, several satellite geometric configurations were considered to analyze aerodynamic control: 3-axis control with feather configuration and 2-axis control with shuttlecock configuration. The analysis was performed by simulating the attitude of the satellite as well as the disturbances affecting the spacecraft. The models implemented to simulate the disturbances were the following: Gravitational gradient torque disturbance, magnetic dipole torque disturbance (magnetic field model IGRF12), and aerodynamic torque disturbances (aerodynamic model DTM2013 and wind model HWM14). The maneuvers analyzed were the following: detumbling or attitude stabilization, pointing and demisability. Different VLEO parameters were analyzed for every geometric configuration and spacecraft maneuver. The results determined which of the analyzed geometric configurations suits better for every maneuver.

Keywords: VLEO, Aerodynamic Attitude Control, Control Algorithms, Gas Surface Interaction, DISCOVERER

1 INTRODUCTION

It is a reality that interest in VLEO is increasing considerably given the advantages of this type of orbit [1]: telecommunications benefit, revision time is improved, optical payloads can provide higher resolution images at lower cost. In addition, there is less space debris in VLEO orbits. Besides, VLEO also offers the possibility to utilise the increased atmospheric density at low altitudes for novel purposes, for example aerodynamics-based control or atmosphere-breathing electric propulsion (ABEP), helping to enable sustained operations in this regime. This is why large companies such as SpaceX are investing heavily in the area. But on the other hand, VLEO missions face problems such as high atmospheric density, which drastically reduces useful life (due to interactions of the gas surface with the free molecular flow) and increases corrosion (produced by atomic oxygen). Gas-surface interactions increase drag forces and aerodynamic pairs, making their operations significantly different compared to satellites flying in LEO orbits.

The effects of drag and lift on a spacecraft have been extensively reviewed in the literature. The interaction between atmospheric particles and spacecraft surfaces is responsible for pairs and aerodynamic forces. In VLEO, the characteristic behavior of the atmosphere with respect to a satellite in orbit is of the free molecular flow type and has important implications when modelling the system [5]. There are several models for modelling gas surface interactions (GSI) in such rarefied environments [6]

This paper was presented at the 17th Reinventing Space Conference, Belfast, November 2019.

and [7]. One of the most widely used GSI models was proposed by Sentman [7]. Several analytical solutions have been tested to perform the analysis of GSI models in the literature: Direct Monte Carlo Simulation (DSMC) [8], panel-based analytical methods [9 and 10] or Monte Carlo test particles (DSMC) [14]. The DSMC simulates collisions of molecules, which accurately model the interaction between atmospheric particles and the satellite surface, but requires large computing resources and time. The panel methods have the advantage of requiring less computing resources, which makes them very agile to be implemented in real time.

The impact of the space environment of VLEO on the useful life of a satellite was previously analyzed by Pulido [11]. Recent research has focused on the analysis of different methods and their application in different scenarios to obtain results [12, 13 and[14], their application in attitude control simulations[15] or the use of drag and lift for maneuvers[16].

The growing interest in the exploitation of very low Earth orbits (VLEO) has given rise to new operational concepts, including the use of the aerodynamic orbit and attitude control methods. Aerodynamic forces and pairs are the main source of perturbation that a spacecraft will experience at these lower altitudes in VLEO. Apart from using traditional attitude control actuators, such as reaction wheels, CMG and magnetorquers, aerodynamic attitude control can also be employed.

A number of attitude control methods using orbital aerodynamic effects have been proposed in the past. In some cases, these methods have been demonstrated in orbit and ultimately used for some operational purpose. Notable examples are the GOCE mission, which used an aerostable geometry to assist the drag compensation propulsion system required to accurately map the Earth's gravitational field, and the ORBCOMM constellation, which used differential drag techniques to assist in the deployment of different satellites in their planned orbital slots.

However, a more complex aerodynamic control has not yet been developed or demonstrated. For Earth observation (EO) applications, the ability to provide accurate and stable pointing in the presence of disrupting forces and pairs is necessary. Maneuverability is also often desired, requiring platform agility and the ability to compensate or reject unwanted aerodynamic pairs. Combinations of aerodynamic control and traditional attitude control actuators can provide the necessary performance, while aerodynamics can also help maintain these actuators, for example through momentum management. The DISCOVERER project is also making a strong effort to research materials that can improve the gas-surface interaction properties (GSI) in the VLEO environment.

In this paper the results of several maneuvers using an aerodynamic control in VLEO are shown. The VLEO environment is described first, as well as the existing disturbances. Two concepts of reference aerodynamic platform to which aerodynamic control methods could be applied have been analyzed: Feather and shuttlecock. Additionally, adjustable aerodynamic control surfaces are detailed, allowing variable aerodynamic control on one or more axes.

Within the context of DISCOVERER, the opportunity to perform in-orbit demonstration of aerodynamic control maneuvers exists using the aerodynamics test satellite SOAR (Satellite for Orbital Aerodynamics Research).

2 MATERIALS AND METHODS

2.1 Environmental models and perturbations

Environment perturbation torques acting on a satellite in orbit includes gravity gradient, solar radiation, aerodynamic torque and Earth's magnetic field. The gravity gradient is the spatial rate of change of gravitational acceleration and it is produced around the centre of mass of the satellite. Solar radiation perturbation is caused by the force created by the transfer of momentum of the absorbed photons to the spacecraft. The aerodynamic torque is originated by the interaction between the surfaces of the satellite and the upper atmosphere particles. It is considered as the main perturbation in VLEO satellites. Finally, the Earth's magnetic field has influence in the motion of a satellite too. The currents in the satellite generate a magnetic dipole that creates a torque in presence of the Earth's magnetic field.

The tool used to run the simulations was Scilab (version 6.0.2) with its graphical modelling tool, Xcos. Scilab is a software tool for numerical computation. It implements a collection of numerical algorithms covering several fields of knowledge, such as aeronautics, thermal and fluid dynamics, signal and image processing, among others. It can be used to solve many aspects of scientific computing problems. Xcos is an open source graphical tool to design models using functional blocks. It provides a palette of basic blocks that can be used to solve differential equations and facilitate object oriented computation. It also facilitates the creation of functional blocks with source code in C, C++ or Fortran. This functionality was used to extend the palette of blocks available in the tool and add all the elements required for simulating VLEO environmental conditions and compute all the disturbances affecting the satellite.

In order to get realistic values of the perturbations affecting the satellite the following models were used:

- Atmospheric model: The Drag Temperature Model DTM2013 [3]
- Earth's magnetic field model: International Geomagnetic Reference Field IGRF12 [2]
- Atmospheric wind: Horizontal Wind Model HWM14 [4].

The Drag Temperature Model (DTM2013) is a semi-empirical model which provides the temperature, density, and composition of the Earth's thermosphere. It is tuned with data provided by CHAMP, GRACE and GOCE spacecraft. This model covers the 200–900 km altitude range and includes information from solar activity. DTM2013 was developed by including data from the DTM2009 model, but incorporates more data from GRACE and GOCE in particular.

The 12th generation of the International Geomagnetic Reference Field (IGRF12) updates the previous IGRF generation with an ultimate main field model for epoch 2010.0, a main field model for epoch 2015.0, and a linear annual predictive secular variation model for 2015.0-2020.0. Fig. 1 shows the magnetic field calculated with IGRF12 model at an altitude of 300 km.

HWM14 is an update to the HWM07 empirical model for horizontal winds in the troposphere, stratosphere, mesosphere, and thermosphere. In the thermosphere, the model consists of two parts: a quiet-time part (without geomagnetic influence) and a geomagnetically disturbed part. It does not consider solar activity dependence.

Wind models are usually focused on the calculation of the

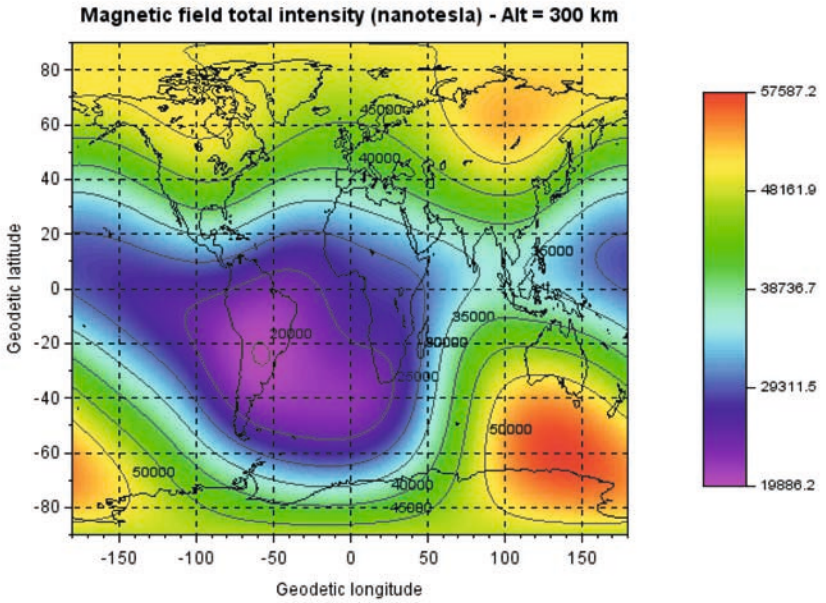

Fig.1 Magnetic field at 300 km.

horizontal components (zonal and meridional). The vertical component of wind velocity, usually, is much lower than the horizontal ones and it is considered negligible. Vertical components are not easily measured. Larsen et al. [17] remark in their study that there are only a few profiles of the vertical winds. The region of interest for VLEO matches the F region of the thermosphere. This region has the highest concentration of free electrons and ions in the atmosphere. A higher temperature increases the concentration of ions due to the reactions produced in the atmosphere. So the solar activity, temperature and the earth field have a great impact in the winds in the thermosphere. The experimental results described by Larsen et al. show different values of the vertical winds in the F region. It shows speeds below 40 m/s or 10 m/s depending on the sources they cite in their study. These measurements are one order of magnitude lower than the horizontal winds that are calculated with the Horizontal Wind Model (HWM14).

Furthermore, the models that provide information about the vertical wind were analysed. GITM [18] and MENTAT [19] are examples of models that fulfil this requirement. If we consider the following:

- The implementation of a wind model is out of the scope of the project
- The disturbances that affect the spacecraft the most are already included in the results presented in this document
- The horizontal wind, that is an order of magnitude higher than the vertical component, is being considered.

We can conclude that we can omit the effects of the vertical wind.

Fig. 1 shows the magnetic field calculated with IGRF12 model at an altitude of 300 km.

Fig. 2 shows the density map calculated using the NRLMSISE-00 model. It shows the values of density at different latitudes all along the day (local solar time).

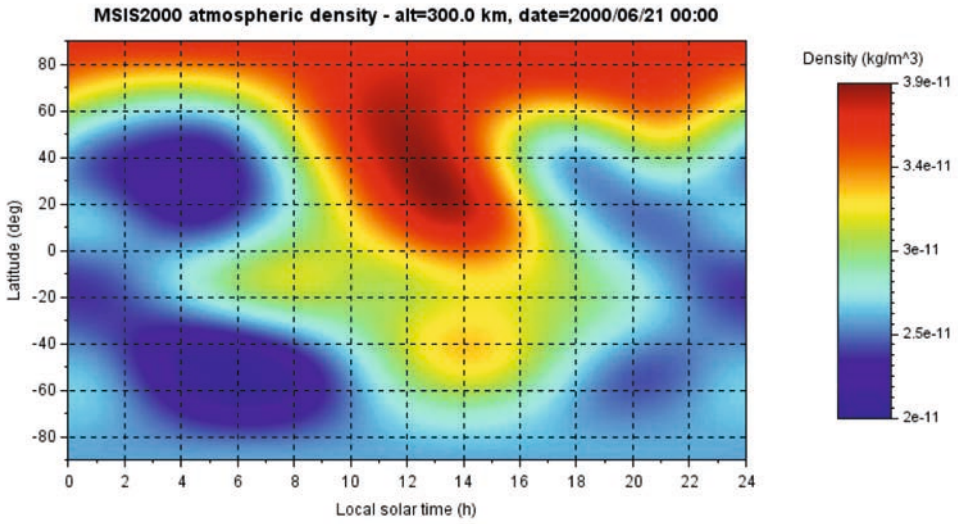

Fig.2 NRLMSISE density map at an altitude of 300 km.

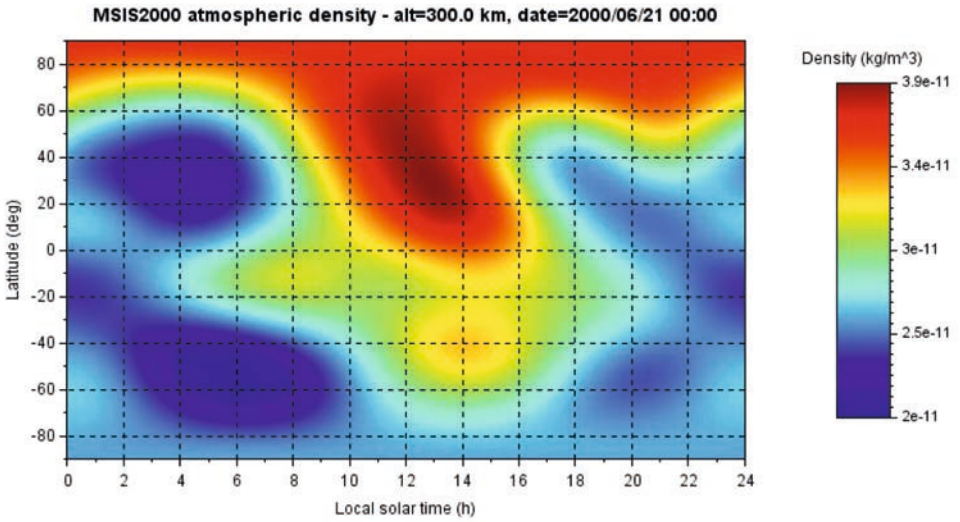

Fig.3 DTM2013 density map at an altitude of 600 km.

Fig.3 shows the density map calculated using DTM2013 model at an altitude of 600 km.

The analysis of the perturbations with models that are more accurate facilitate the estimation of more realistic environmental perturbations. The perturbations were computed as follows:

- Magnetic torque $\vec{T}_{mag_q}$ (Nm):

$$\vec{T}_{mag_q} = \vec{m}_q \times \vec{B}_q \tag{1}$$

where where $\vec{m}_q$ (Nm/T) is the magnetic dipole of the satellite and $\vec{B}_q$ (T) is the magnetic field of the Earth.

- Gravity gradient torque $\vec{T}_{gravity}$ (Nm):

where μ is the gravitational constant of the Earth, which can be calculated as $\mu=GM$, with G the universal gravitational constant (6.674×10^{-11} Nm^2/kg^2) and M the mass of the Earth (5972×10^{24} kg); R is the distance from the centre of the Earth to the orbit of the satellite.

$$\vec{T}_{gravity} = \frac{3\mu}{R^2}\begin{bmatrix}(I_{zz}-I_{yy})b_1c_1\\(I_{xx}-I_{zz})a_1c_1\\(I_{xx}-I_{zz})a_1c_1\end{bmatrix} \tag{2}$$

where I_{xx}, I_{yy} *and* I_{zz} the diagonal elements of the inertia matrix (kg/m^4) and a_1, b_1 and c_1 coefficients defined as follows in quaternions notation:

$$\begin{aligned} a_1 &= 2q_1q_3 - 2q_2q_4 \\ b_1 &= 2q_2q_3 + 2q_1q_4 \\ c_1 &= 2q_4^2 + 2q_3^2 - 1 \end{aligned} \tag{3}$$

- Aerodynamic torque $\vec{T}_{aero}$ (Nm):

$$\vec{T}_{aero} = \sum_{i=1}^{n}(\vec{F}_{D_i} + \vec{F}_{L_i}) \times \vec{r}_i \tag{4}$$

being $\vec{r}_i$ the position vector between the geometric centre of the satellite and the centre of pressure of the panel and $\vec{F}_{L_i}$ and $\vec{F}_{D_i}$ lift force and the drag force for each panel respectively and the aerodynamic force $\vec{F}_{aero}$ (N) as follows:

$$\vec{F}_{aero} = \sum_{i=1}^{n}(\vec{F}_{D_i} + \vec{F}_{L_i}) \tag{5}$$

where $\vec{F}_{L_i}$ (N) and $\vec{F}_{D_i}$ (N) are defined as:

$$F_{D_i} = \frac{1}{2}\rho C_d \vec{V}_{aero}^2 A_i \tag{6}$$

$$F_{L_i} = \frac{1}{2}\rho C_l \vec{V}_{aero}^2 A_i \tag{7}$$

being C_l the lift coefficient, C_d the drag coefficient, A_i the panel surface (m^2), ρ the density (kg/m^3) and $\vec{V}_{aero}$ the aerodynamic velocity (m/s):

$$\vec{V}_{aero} = \vec{V}_{orb} + \vec{V}_{wind} \tag{8}$$

where $\vec{V}_{orb}$ is the orbital velocity (m/s) and $\vec{V}_{wind}$ the wind velocity (m/s).

As stated before, aerodynamic forces are the main disturbances acting on a spacecraft in VLEO. A panel method implementation was developed and used in this work in order to calculate aerodynamic forces affecting the spacecraft. In this method the spacecraft surface was modelled as a composition of simple panels. The forces and torques produced by GSI were calculated for each panel and after that they were combined to obtain the overall component. The gas-surface interaction was modelled by using Sentman's model equations [7]. The dimensionless drag coefficient Cd can be calculated as follows:

$$C_d = \left\{\frac{P}{\sqrt{\pi}} + QZcos(\theta) + \frac{cos(\theta)}{2}\frac{V_{re}}{V_{inc}}(\sqrt{\pi}Zcos(\theta) + P)\right\}\frac{A}{A_{ref}} \tag{9}$$

$$C_l = \left\{GZsin(\theta) + \frac{sin(\theta)}{2}\frac{V_{re}}{V_{inc}}(\sqrt{\pi}Zcos(\theta) + P)\right\}\frac{A}{A_{ref}} \tag{10}$$

$$P = \frac{1}{S}e^{-S^2cos^2(\theta)} \tag{11}$$

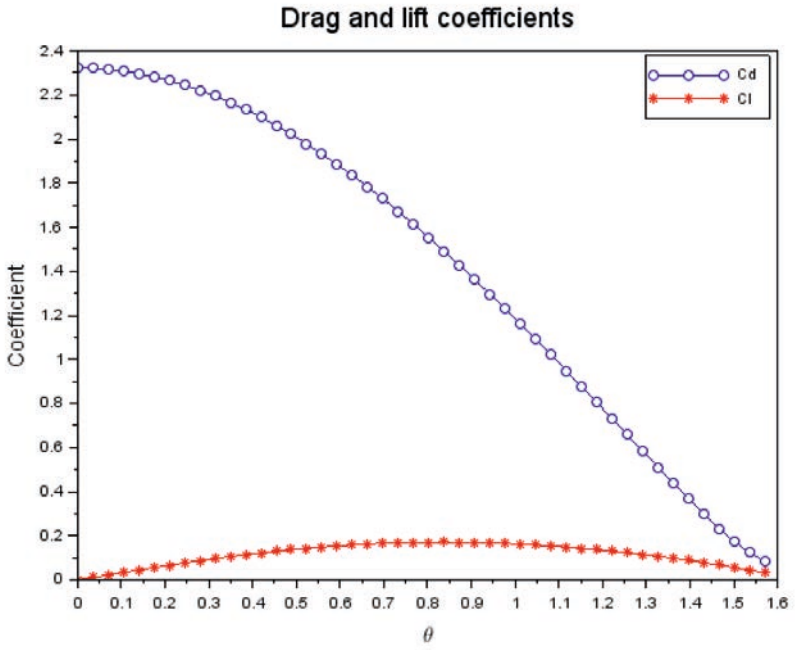

Fig.4 Drag and lift coefficients.

$$G = \frac{1}{2S^2} \quad (12)$$

$$Q = 1 + G \quad (13)$$

$$Z = 1 + \mathrm{erf}(S\cos(\theta)) \quad (14)$$

$$\frac{V_{re}}{V_{inc}} = \sqrt{\frac{1}{2}\left[1 + \sigma_a\left(\frac{4RT_W}{V_{inc}^2} - 1\right)\right]} \quad (15)$$

where, C_d is the dimensionless drag coefficient and C_l is the dimensionless lift coefficient. θ is the angle (in radians) between the velocity vector and the normal vector to the surface (0 *rads* indicate that the surface is perpendicular to the flux and π/2 when they are parallel), S is the dimensionless ratio between the orbital velocity, $V\infty$ (m/s), and the most probable random speed of the molecules, C (m/s). This is defined as:

$$C_m = \sqrt{2\frac{R}{m}T_i}$$

in which R is the ideal gas constant ($J/(mol\ ^oK)$), m (kg/mol) is the mean atomic gas mass of the molecules constituting the atmosphere and Ti (^oK) is the temperature of the incident particles. Hence:

$$\frac{V_\infty}{C_m}, V_{re}\ (m/s) \text{ and } V_{inc}\ (m/s)$$

are the velocities of the reflected and the incident molecules, T_w (^oK) is the temperatures of the surface wall and A (m²) is the area of the panel surface A_{ref} (m²) is a reference area, which was defined as follows for the calculations carried out in this paper

i) for the case of 1U, 1.5U, 2U and 3U CubeSats, the reference area was the area of a face of a 1U CubeSat, or its base, (10cm x 10cm),

ii) for the case of the 12U, the reference area was 10cm x 20cm (the base of the CubeSat),

and iii) for the 8U, 12U and 16U, the reference area was 20cm x 20cm (the base of the CubeSats). See Fig. 2. Fig. 3 shows the 1U geometry considered for the calculations.

For the calculations the values considered for the thermal accommodation coefficient and surface temperature were:

$$\sigma_a = 0.95 \text{ and } T_W = 400K$$

Fig. 4 shows the variation of the drag and lift coefficients with variations of θ. The results indicate that the drag coefficient is always higher than the lift coefficient, and that with low values of θ, the drag is several orders of magnitude higher than the lift.

In order to establish a comparison between a satellite flying at LEO and VLEO two different cases were considered: 700 km and 350 km orbits. For calculations, the launch date was 3 April 2012 at 18:00:00. The orbit parameters are defined in Table 1.

Shuttlecock and Feather configurations (see Fig. 5) were selected for comparison in this work. The length of the fins is the same as that of the Feather configuration (90 cm), so that

TABLE 1 Orbits used in simulations

	Altitude (km)	**Inclination** (degrees)	**Arg.Perigee** (degrees)	**MItan** (h)	**Eccentricity**
LEO	700	50	90	12	0.001
VLEO	350	50	90	12	0.001
	Altitude (km)	**Inclination** (degrees)	**Arg. Perigee** (degrees)	**MItan** (h)	**Eccentricity**
LEO	700	50	90	12	0.001

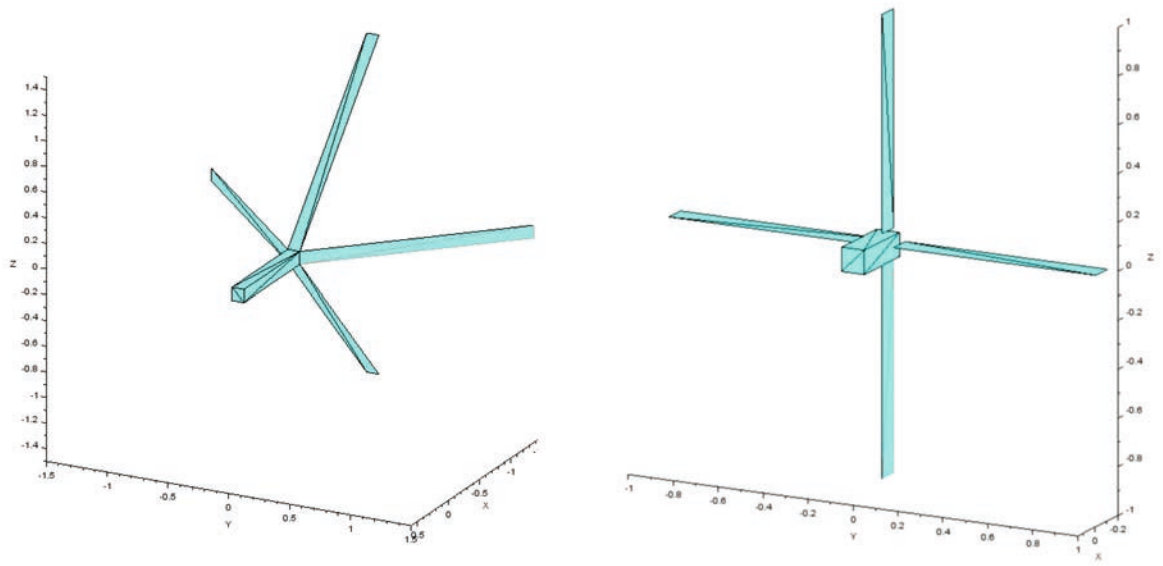

Fig.5 Shuttlecock (left) and Feather (right) configurations.

both simulated configurations are equal in terms of aerodynamic area and therefore comparable. The main body of both spacecraft is a standard 3U CubeSat.

In attitude control, combinations of synergetic aerodynamic-based control and traditional attitude actuators (reaction wheels) are typically selected to investigate the development of pointing and trim maneuvers. Aerodynamic control is also chosen to perform the momentum management of the reaction wheel with the intention of avoiding saturation of the actuators in the presence of disturbing environmental torques.

In order to perform the simulations of the maneuvers analyzed in this paper (stabilization and pointing), PID through a Jacobian formulation was selected. A range of other control methods were considered, but since the main goal of this paper is to demonstrate de feasibility of the aerodynamic, a robust algorithm was chosen to the detriment of efficiency.

3 RESULTS

Fig. 6a shows the density of the atmosphere at 700km altitude and Fig. 6b shows the density of the atmosphere at 350km altitude along the orbits. The value of the density changes in function of the sun radiation in the position of the orbit. In both figures, between 40° and 70° inclinations the density of the atmosphere reached the highest values, more specifically, at 700km the maximum density reached 6.05·10-14 kg/m^3 at -70° of inclination, and the minimum density was 1.28·10-14 kg/m^3 at 128° of inclination; and for VLEO orbit, the maximum density reached the maximum density value of 1.17·10-11 kg/m^3 at a longitude of -63°, while the minimum density was 4.35·10-11 kg/m^3 at 128° longitude. Notice that at VLEO the density of the atmosphere is three orders of magnitude higher that at LEO.

Fig. 7a shows the two horizontal components of atmospheric wind at LEO and VLEO (Meridional and Zonal). It is remarkable that both components are quite similar in shape at LEO and VLEO. Besides, the wind rises at longitudes corresponding to the eclipse part of the orbit (between -50° and 150° longitude). However, even though the wind components are similar at LEO and VLEO, notice that at VLEO the density of the atmosphere is higher. This leads to a higher interaction of the atmosphere molecules with the surfaces of the satellite.

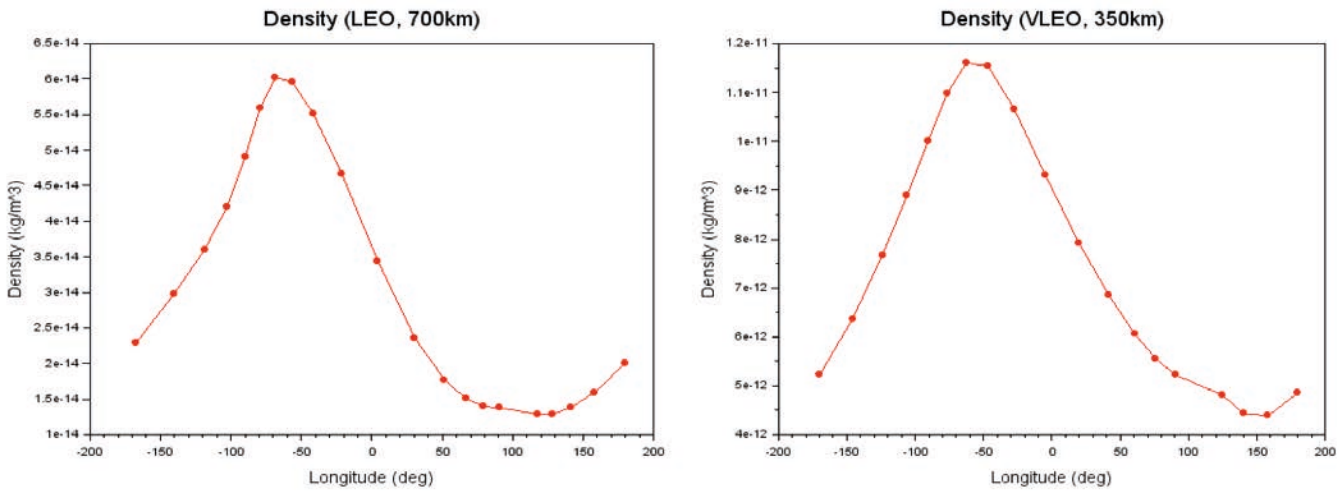

Fig.6 Atmospheric density (a) and atmospheric density (b) in VLEO.

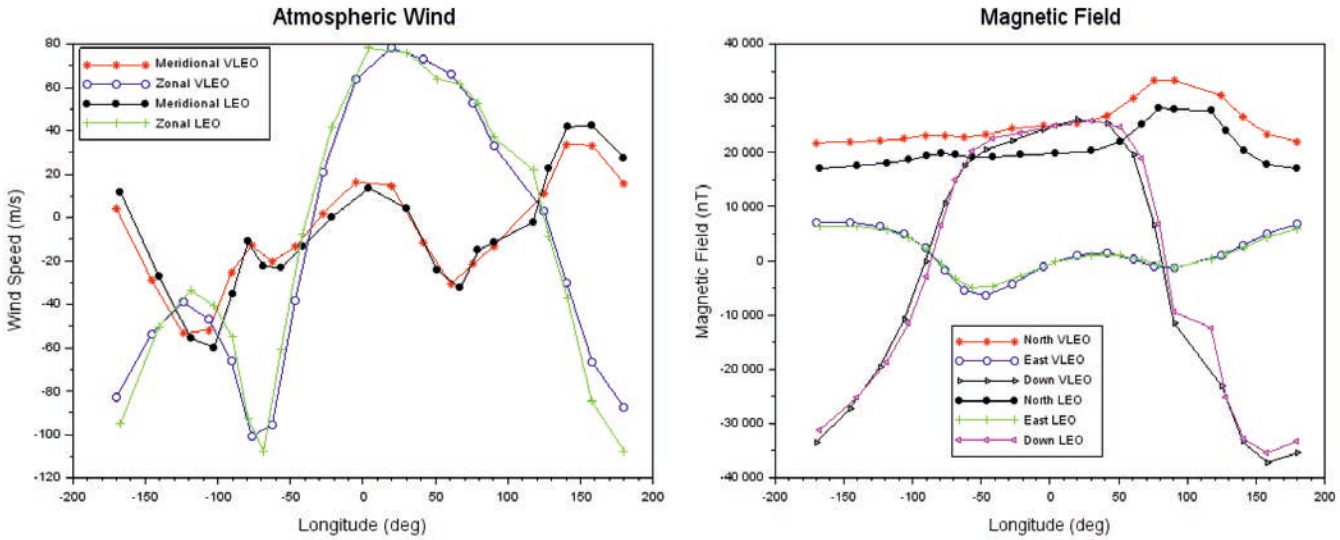

Fig.7 Magnetic field (a) and Horizontal wind (b) components in LEO and VLEO.

Fig. 7b depicts the three components of the magnetic field at LEO and VLEO (North, East and Down). Notice that at LEO and at VLEO the components of the magnetic field are quite similar in shape, and in the case of East and Down components are almost coincident. However, in the case of the North component, at VLEO has higher magnitude because it is closer the surface of the Earth.

The geometry of the spacecraft and the material which is in contact with the atmosphere in VLEO are aspects of major importance. Aerodynamic forces and torques can be used to carry out attitude control and stabilization maneuvers. In order to show this aerodynamic stabilization and pointing maneuvers with shuttlecock and feather configurations were simulated to analyze the capabilities of these systems when only aerodynamic interaction is taking place during operation. The simulated external torques were the following: the gravity gradient, dipole magnetic field, aerodynamic torque and the internal torques generated by the mobile parts. The orbit parameters are defined in Table 2. The dimension of the fins for both shuttlecock and feather configuration was 90cm x 10cm.

Fig. 8 shows the attitude control of the 1U satellite carried out with reaction wheels. The initial conditions of the angular velocity were 0.05 rad/s, -0.54 rad/s and 0.19 rad/s for x, y and z components respectively. Notice that in both cases, LEO (7a) and VLEO (7b), the behaviour is similar. This is because the magnitude of the aerodynamic torques is $3.7 \cdot 10^{-9}$ Nm for the 1U satellite and the reaction wheels maximum applicable torque is $2.3 \cdot 10^{-3}$ Nm, this is three orders of magnitude higher, what means that the reaction wheels easily compensate the torques.

TABLE 2 Orbit parameters

Type of orbit	Altitude (km)	Inclination (degrees)	Argument of Perigee (degrees)	MItan (hh:mm)	Eccentricity
VLEO	350	50	90	12	0.001

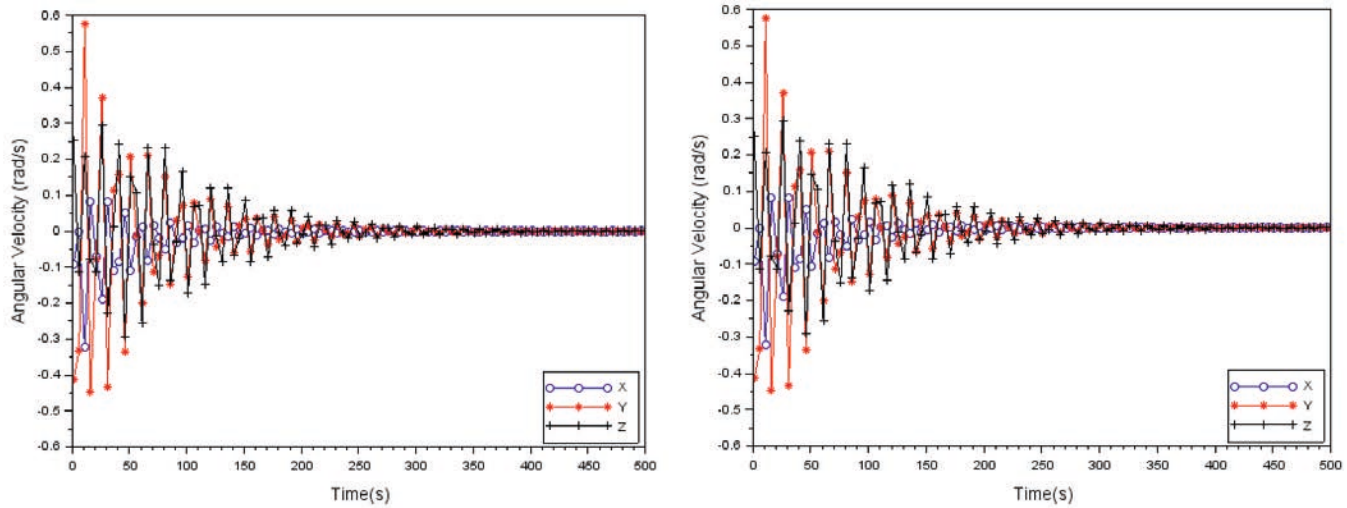

Fig.8 Attitude control of the 1U CubeSat satellite in (a) LEO (700 km) and (b) in VLEO (350 km).

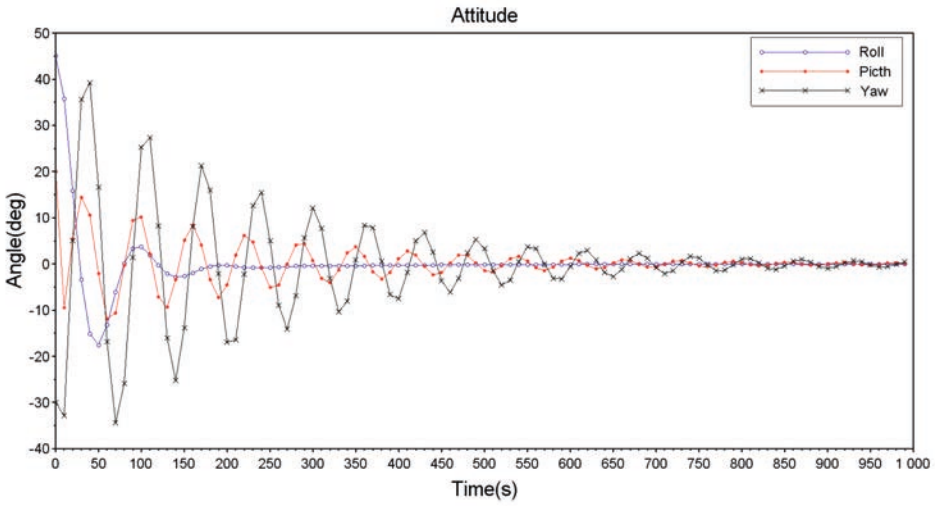

Fig.9 Attitude stabilization for feather configuration (3 axis control).

The attitude stability of the feather configuration was studied in three axes (Fig. 9). The settling time was considered the moment when the difference between the signal and the reference is lower than one degree. The maximum maneuverability is reached in roll axis, with a settling time of 172 seconds (2.87) minutes). Pitch and yaw axes behaved similarly and showed a settling time of 607 seconds (10.11 minutes) and 812 seconds (13.53 minutes), respectively. In this configuration, mainly lift is used in the maneuvers.

Table 3 shows the results obtained for a pointing maneuver. The target angle was 15 degrees. The settling time and the overshoot are presented for different accommodation coefficients, which depend on the material used for the fins, the temperature and the roughness of the surface. The higher was the accommodation coefficient the higher was the settling time and the overshoot.

The same analysis was carried out for the shuttlecock configuration. Fig. 10 shows the results of the attitude stabilization for that geometry. In this case, drag is mainly used in the maneuvers. The stabilization is faster than with the feather configuration. However, this configuration has lack of roll controllability. It would need the use of a reaction wheel or magnetorquers to have controllability in the roll axis. For instance, pitch and yaw axes had a settling time of 183 seconds (3.05 minutes) and 197 seconds (3.28 minutes), respectively: one order of magnitude less than with feather configuration: 10.11 minutes and 13.53 minutes respectively.

TABLE 3 Influence of the accomodation coefficient on pointing maneuver

Accommodation coefficient	Settling time (s)	Overshoot (%)
0	4281	32.73
0.2	5426	32.86
0.4	9022	33.01
0.6	22513	33.13
0.8	68319	36.06
0.95	-	-

Table 4 shows the comparison of the pointing maneuver for both configurations feather and shuttlecock with different pointing angles. The settling time was lower for the shuttlecock configuration but the overshoot was higher. In the case

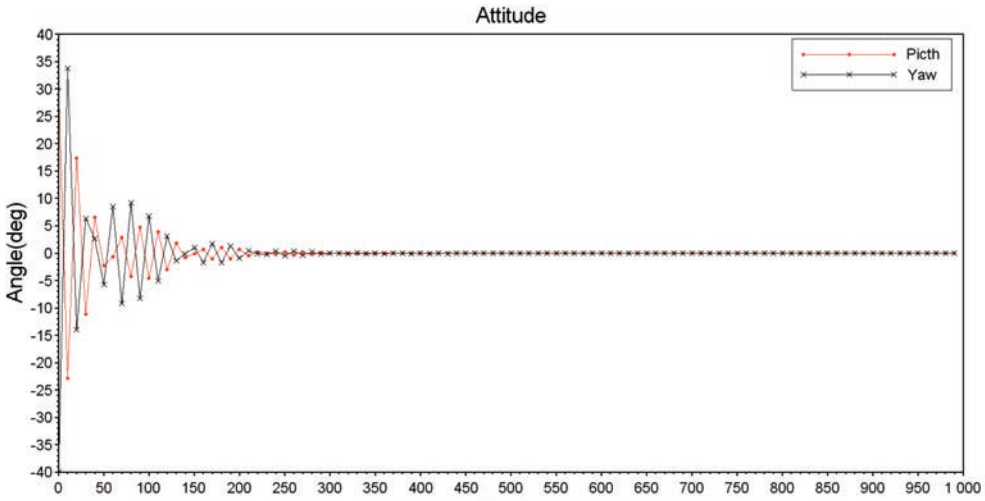

Fig.10 Attitude stabilization for shuttlecock configuration (2 axis control).

TABLE 4 Comparison of pointing maneuver for feather and shuttlecock configurations

	Feather		Shuttlecock	
Pointing Angle	Settling Time	Overshoot(%)	Settling Time	Overshoot(%)
5	3523	37.8	253	79.3
10	3271	35.7	261	77.8
15	4116	29.5	272	73.7
20	-	-	279	69.1
25	-	-	312	62.1
30	-	-	433	51.5
35	-	-	673	42.1
40	-	-	-	-

of the feather configuration the range of the pointing angles was lower than in the shuttlecock configuration. From a pointing angle of 18 degrees this configuration cannot reach a steady state using a PID controller for the fins.

Fig. 12 and Fig. 13 show the apogee and perigee altitude along the lifetime of the 1U satellite for LEO and VLEO respectively. No deorbiting manoeuvres were considered. Besides, the satellite was kept with a constant attitude along the orbit: one of the faces was perpendicular to the tangential direction of the orbit. Notice that the satellite re-enters after 40 years in the LEO scenario and 73 days in the case of the VLEO.

Fig. 14 overleaf depicts the time that different CubeSat configurations require to re-enters when flying at different altitudes. To establish the comparison, the mass to area ratio was considered. This is the relation between the frontal area of the satellite and its mass. All the satellites were considered to be flying with constant attitude, in which the frontal face was perpendicular to the tangential direction of the orbit. The 1U CubeSat has a mass to area ratio of 0.01, 2U and 8U have the same mass to area ratio, which is 0.005; 3U, 6U and 12U have the same mass to area ratio, which is 3.33·10-3, and 16U has a mass to area ratio of 2.5·10-3. The picture shows that the 1U satellite is the most unfavourable case because it has the higher mass to area ratio, while the 16U is the most favourable case among all the configurations analysed.

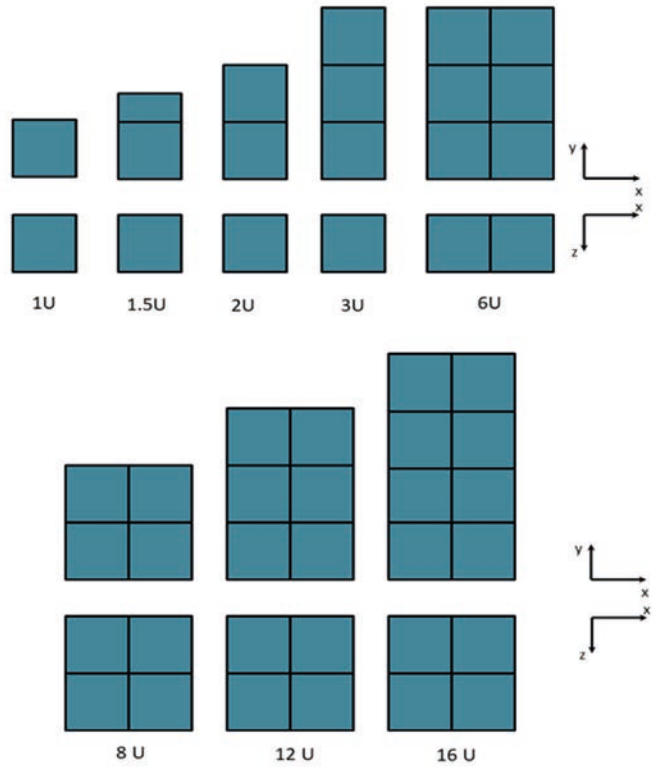

Fig.11 CubeSats sizes used in the calculations.

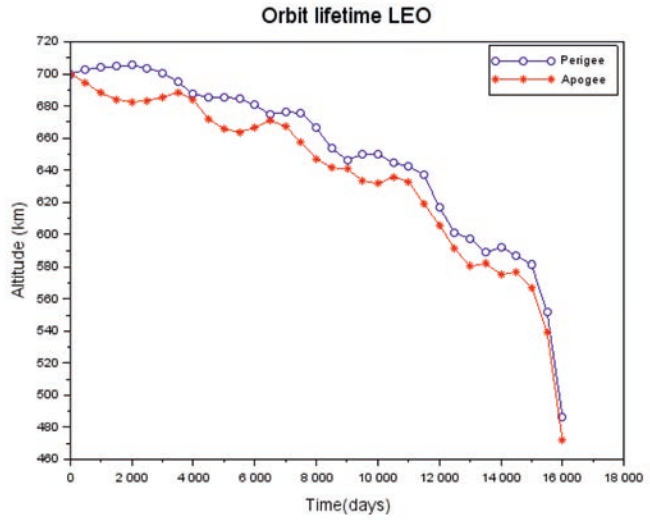

Fig.12 Orbit lifetime for a 1U CubeSat satellite in LEO (700 km).

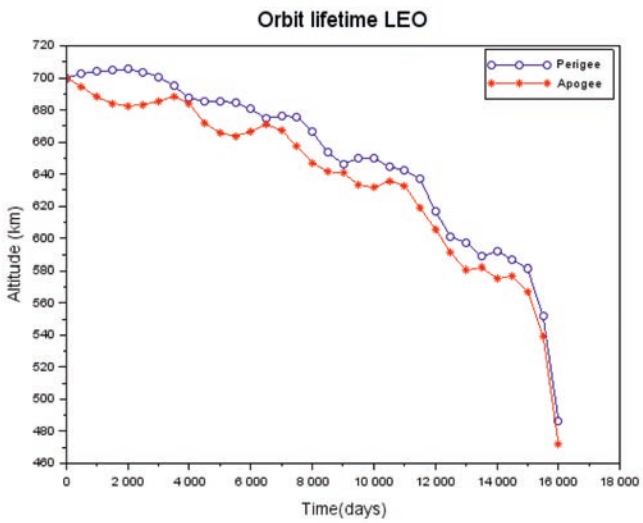

Fig.13 Orbit lifetime for a 1U CubeSat satellite in VLEO (350 km).

Since the requirements of demisability are to fall into low atmosphere before 25 years from the launch, it can be deduced from Fig. 10 that all CubeSat configurations will achieve this by default. This means that the Feather and the Shuttlecock configuration analysed here will also achieve this requirement, since both have a worst mass to area ratio than a conventional 3U.

4 CONCLUSIONS

These results show that it is feasible to perform some manoeuvres in VLEO using only aerodynamic actuators. Both Shuttlecock and Feather demonstrated good behaviour in passivation manoeuvres, but show certain limitations in terms of the settling time and the maximum range that can be reached in pointing manoeuvres. Shuttlecock also does not have a good control on the roll axis, which means that in most cases the spacecraft should need at least one reaction wheel to complement the aerodynamic fins for roll axis controllability.

In order to have complete control in pointing manoeuvres it is therefore necessary to have reaction wheels with control on all three axes. In this case, the capabilities of the aerodynamic fins allow a momentum management system to be set up so as to avoid saturation of the reaction wheels.

The results presented in this paper remark the importance of the geometry and the material used to build a spacecraft to take advantage of the environment in VLEO orbits, where the atmospheric fluid behaviour has to be considered as a free molecular flow, having important implications when modelling the system. Aerodynamic forces and torques can be used to carry out some attitude control and stabilization manoeuvres. As major result, aerodynamic stabilization and pointing manoeuvres were showed to be feasible on VLEO using aerodynamic surfaces.

Acknowledgments

This work has received funding from the European Union's Horizon 2020 research and innovation programme, DISCOVERER project, under grant agreement No ID 737183.

REFERENCES

1. J. Becedas, G. González, R.M. Domínguez et al. 2018. "Aerodynamic technologies for Earth Observation missions in VLEO." *16th Reinventing Space Conference*, 2018
2. E. Thébault, C.C. Finlay, C.D. Beggan, P. Alken et al. "International Geomagnetic Reference Field: the 12th generation." Earth, Planets and Space 67-79. doi:10.1186/s40623-015-0228-9, 2015.
3. S. Bruinsma, "The DTM-2013 thermosphere model." Journal of Space Weather and Space Climate, 5, A1. doi: https://doi.org/10.1051/swsc/2015001, 2015.
4. D. P. Drob, J. T. Emmert, J. W. Meriwether, J. J Makela, E. Doornbos, M. Conde and J. D. Huba, "An update to the Horizontal Wind Model (HWM): The quiet time thermosphere." *Earth and Space Science*, 2(7), 301-319, 2015.
5. S. A. Schaaf, and P. A. Chambre, *Flow of Rarefied Gases*. Princeton Aeronautical Paperbacks, Princeton University Press, 1961.
6. R. Schamberg, *A new analytic representation of surface interaction with hypothermal free molecule flow with application to neutral-particle drag estimates of satellites*. Technical Report RM-2313, RAND Research Memorandum, 1959.
7. L. H. Sentman, *Free Molecule Flow and its Application to the Determination of Aerodynamic Forces*. Lockheed Missiles and Space Co. Inc. Technical report LMSC-448514. Sunnivale. California. Pg.111, 1961.
8. G. A. Bird and J. M. Brady, *Molecular gas dynamics and the direct simulation of gas flows*. Oxford: Clarendon press. Vol. 5. 1994.
9. K. Moe and M, M. Moe, Gas–surface interactions and satellite drag coefficients. Planetary and Space Science, 53(8), 793-801. doi:10.1016/j.pss.2005.03.005, 2005.
10. M. L. Gargasz, Optimal Spacecraft Attitude Control Using Aerodynamic Torques. No. AFIT/GA/ENY/07-M08. Air Force Institute of Technology, Ohio, 2007.
11. C. L. Pulido, *Aerodynamic Lift and Drag Effects on the Orbital Lifetime Low Earth Orbit (LEO) Satellites*. University of Colorado Boulder, 2007.
12. A. Walker, P. Mehta, & J. Koller, "Drag coefficient model using the cercignani–lampis–lord gas–surface interaction model." *Journal of Spacecraft and Rockets*, 51(5), 1544-1563, 2014.
13. P. M. Mehta, C. A. McLaughlin, and E. K. Sutton, "Drag coefficient modelling for grace using Direct Simulation Monte Carlo." *Advances in Space Research*, 52(12), 2035-2051, 2013.
14. X. Jin, F. Huang and X. Cheng, "Test Particle Monte Carlo Simulation of the Interaction of Two Parallel Flat Plates in Free Molecular Flow Regime." *Procedia Engineering*, 126, 675–679. doi:10.1016/j.proeng.2015.11.263, 2015.
15. J. Virgili Llop, H. C. Polat, and M. Romano, "Attitude Stabilization of Spacecraft in Very Low Earth Orbit by Center-of-Mass Shifting." *Frontiers in Robotics and AI*, 6, 7, 2019.
16. C. Traub, F. Romano, T. Binder, A. Boxberger, G. H. Herdrich, S. Fasoulas, and N. H. Crisp, "On the exploitation of differential aerodynamic lift and drag as a means to control satellite formation flight." *CEAS Space Journal*, 1-18, 2019.
17. Larsen, M. F., and J. W. Meriwether, "Vertical winds in the thermosphere." *Journal of Geophysical Research: Space Physics* 117.A9, 2012.
18. A. J. Ridley, Y. Deng, and G. Toth, "The global ionosphere–thermosphere model." *Journal of Atmospheric and Solar-Terrestrial Physics* 68.8 pp839-864, 2006.
19. P. B. Dandenault, "MENTAT: A new wind model for Earth's thermosphere." *Journal of Geophysical Research: Space Physics* 123.8 pp7124-7147, 2018.

Received 28 January 2020 **Approved** 26 March 2020